Materials and Design 200 (2021) 109451

Contents lists available at ScienceDirect

Materials and Design

journal homepage: www.elsevier.com/locate/matdes

Adhesion evaluation of thin films to dielectrics in multilayer stacks: A comparison of four-point bending and stressed overlayer technique.

A. Lassnig [a,*,1], B. Putz [a,b,1,*], S. Hirn [c], D.M. Többens [d], C. Mitterer [c], M.J. Cordill [a]

[a] Erich Schmid Institute of Materials Science, Austrian Academy of Sciences, Jahnstrasse 12, Leoben 8700, Austria
[b] Empa, Swiss Federal Laboratories for Materials Science and Technology, Feuerwerkerstrasse 39, 3602 Thun, Switzerland
[c] Department of Materials Science, Montanuniversität Leoben, Franz-Josef-Strasse 18, 8700 Leoben, Austria
[d] Helmholtz-Zentrum Berlin für Materialien und Energie (HZB), Albert-Einstein-Str. 15, 12489 Berlin, Germany

HIGHLIGHTS

- A model multimaterial stack was designed to integrally test critical interfaces in microelectronic devices.
- Using 4 point bending the weakest interface, WTi-BPSG, was identified revealing an energy release rate of (9.4± 0.6) J/m^2.
- The WTi-BPSG adhesion was also determined using a stressed overlayer on top of WTi leading to the mixed mode adhesion energy (10.1±1.0) J/m^2.
- XRD measurements of the WTi revealed similar stresses regardless of layer setup, allowing a comparison of these test techniques.

GRAPHICAL ABSTRACT

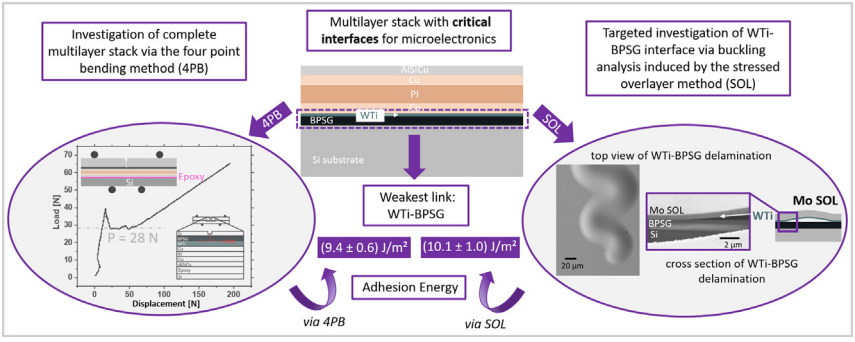

ARTICLE INFO

Article history:
Received 6 September 2020
Received in revised form 1 January 2021
Accepted 4 January 2021
Available online 7 January 2021

Keywords:
Brittle-ductile interface
Four-point bending
Adhesion
Stressed overlayer

ABSTRACT

Assessing the interfacial strength of multilayered structures is crucial to ensure the reliability of such components. Two widely used tests, four-point bending (4PB) and the stressed overlayer (SOL) technique, are juxtaposed and employed in this study to determine adhesion of WTi on borophosphosilicate glass (BPSG) implemented in a model multilayer material stack with representative materials encountered in microelectronic applications including silicon, ductile metallic films and soft polyimide layers. The applicability and reproducibility of both methods is discussed in this paper including a detailed analysis of the stress evolution of the delaminating WTi using X-ray diffraction. While both adhesion measurement techniques reveal comparable adhesion energies for the WTi-BPSG interface, namely (9.4 ± 0.6) J/m^2 and (10.1 ± 1.0) J/m^2 for 4PB and SOL, respectively, we come to the conclusion that 4PB allows to integrally test the entire stack on a larger scale and SOL allows to determine the weakest site of the interface on a local scale. Both suggested methods are promising for future sub-micrometer thin film designs in complex multilayered structures since they are easy to perform and allow for a good statistical output of the results.

1. Introduction

Interface quality is of utmost importance to ensure reliable microelectronic devices. The downscaling of the used materials imposes many novel challenges on the production side, one of them being

* Corresponding authors.
E-mail addresses: alice.lassnig@oeaw.ac.at (A. Lassnig), barbara.putz@empa.ch (B. Putz).
[1] Equally contributing.

https://doi.org/10.1016/j.matdes.2021.109451

increased difficulty to determine adhesion of very thin films quantitatively. The needs towards a reliable evaluation technique are: reproducibility, comparability, cost and time efficiency.

A variety of adhesion techniques are available to either qualify or quantify the interface strength. Qualitative methods, such as peel [1] or tape tests [2], are fast and easy to perform and widely applied, allowing a ranking or assessment of interfaces based on a pass/fail criterion. Calculation of adhesive strength from peel test data requires the uniform delamination of a single interface during peeling, which can then be related to a plateau in the load/displacement curve. However, often only simple systems (single layers) fulfill that requirement. Critics also stress the fact that the peeling force not only causes interfacial delamination but also plastic deformation in the peeled layers [3]. Quantitative techniques yielding adhesion energies (J/m^2) typically require more complex instrumentation and theoretical models for analysis. Some techniques, including four point bending (4PB) [4–8], bulge or blister tests [9], measure adhesion values averaged over a large interfacial area. Other analysis techniques, such as spontaneous or nanoindentation-induced delamination [10,11] with and without compressively stressed overlayers (SOL) [11,12] or in situ micro bending-beam techniques [13–18] yield local adhesion values, allowing one to conduct spatially resolved adhesion mapping measurements [19]. For some techniques, the influence of sample preparation (focused ion beam damage, change of stress state) on the interfacial strength also needs to be considered. While in situ tests under the electron beam allow to directly observe interface delamination and, if successful, unravel mechanisms accompanied with the delamination, their main drawback is that they are experimentally challenging as they require time-consuming sample preparation and tailored geometries. Thus, only few bending beams can be tested per interface, yielding a poor statistical output. Interface adhesion measurements via in situ bending beam experiments conducted under the TEM proposed by Völker et al. [16] were only feasible for weak interfaces (interface fracture energy 1–1.4 J/m^2) but could not be applied to interfaces with substantially higher interface fracture energies.

In the following study, we report the adhesion of WTi on borophosphosilicate glass (BPSG) within a multilayer materials stack commonly encountered in the microelectronics industry. BPSG is a state-of-the-art dielectric and WTi serves as a diffusion barrier and adhesion promotor between BPSG and the conducting Cu layers, which serve as metallization. Multilayered thin films are implemented in several microelectronics structures featuring layers with highly disparate physical properties (brittle ceramics and semiconductors, ductile metal films, soft polymers). It is assumed that not only each individual layer's performance depends on the isolated physical properties, but also an interplay of each neighboring layer determines the overall reliability of the material stack. Of main concern is the detection and quantification of the weakest interface present in the stack. Adhesion of Cu-BPSG [20,21] versus WTi-BPSG [22,23] has been studied as a function of W content, WTi thickness and annealing treatments. In this work, we use two different measurement techniques, namely 4PB and spontaneous delamination with stressed overlayers (SOL) to determine the quantitative adhesion energy of the same WTi - BPSG interface. 4PB allows testing of the complete multilayer stack. Based on our results we can exemplify how the arrangement of individual layers can influence the crack propagation path, prohibiting identification of the overall weakest interface and instead determining adhesion energy of a configurational weakest link. In contrast, the stressed overlayer technique [10,11,24] enables testing of the same interface in a more simple bi-layer geometry. Comparison of the different results allows for a discussion about suitability and the origins of potential differences in the obtained adhesion values.

Residual stresses are inevitable in thin film structures and highly influence the thin film properties and adhesion [25]. These stresses either originate from the deposition process or arise in-operando from exposure of the devices to elevated temperatures leading to stresses due to thermal mismatch of individual components. Along with the adhesion method comparison (4PB vs. SOL), a detailed description of the stress evolution in the WTi layer depending on the number of additional layers is presented. The combination of the results provides insights into the adhesive interplay of neighboring layers in multilayer stacks and can help design reliable material stacks for microelectronics applications.

2. Materials and experimental methods

2.1. Materials

For this study, a representative multilayer stack composed of different materials with highly distinct physical properties that are standardly encountered in microelectronics was designed. The design includes a multitude of critical interface types (brittle-brittle; brittle-ductile and metal-polymer), which pose reliability challenges in microelectronics devices. The multilayer is composed of the following materials: Si as semiconductor material substrate (thickness $h = 725\ \mu m$) followed by BPSG (1.5 μm, annealed), a commonly used dielectric. A thin WTi layer (50 nm, W with 16 at. % Ti) was subsequently deposited and acts as diffusion barrier and adhesion promoter [22] between the BPSG and a magnetron sputtered Cu (600 nm) metallization layer. A 13μm spin coated polyimide layer (PI, 13 μm), extensively used in microelectronics manufacturing and packaging as passivation layers, dielectrics, or insulator layers in multilayer structures, was then added followed by sputter deposited Cu (600 nm) and a sputter deposited 500 nm thick AlSiCu alloy as the top layer. The interfaces between Cu and PI is challenging [26] and widely encountered for rigid and flexible electronics applications and the Cu-AlSiCu interface is often critical in wire bonding interconnects [27]. A schematic of the original stack is shown in Fig. 1b. For adhesion analysis the stack had to be modified for both quantification methods: i) for 4PB into notched bending bars (Fig. 1a) and ii) for spontaneous delamination via a Mo SOL after an HNO_3 etch step into the SOL geometry (Fig. 1c). Details about the modifications will be given in the related paragraphs. To facilitate comparison between all three geometries the 4PB setup is depicted under a 180° rotation as compared to actual testing conditions (Fig. 2a).

2.2. Four-Point bending (4PB)

Adhesion of the WTi-BPSG interface was evaluated with the 4PB approach following Ma et al. [28,29]. A schematic illustrating the experimental setup and the sample geometry is shown in Fig. 1a (180° rotation compared to testing conditions – inset Fig. 2a – to facilitate comparison to original and SOL multilayer). 4PB beams were prepared following the procedure reported by Völker et al. [30]. The 725 μm thick Si (100) wafers were coated with the layer stack described above and subsequently cut into the 4PB geometry (lateral dimension: width $b = 7$ mm; length $= 40$ mm) using a wafer saw with a diamond cutting wheel. Notches (width 36 μm, depth 500 μm) were cut centrally into the Si side also using a wafer saw. To create the 4PB beams the notched samples were glued to pure Si (100) counterparts (uncoated and unnotched) with EPO-TEK 375 epoxy. After curing the epoxy for 8 h at 100 °C in vacuum of about 1×10^{-3} Pa, the edges of the samples were mechanically polished to remove epoxy residues and to obtain flat surfaces.

4PB was performed on a Kammrath & Weiss bending module with a crosshead speed of 0.1 μm/s. A valid experiment [23,31] requires symmetric kinking of a crack from the notch into both sides of the interface of interest and a corresponding load plateau in the load-displacement curve (Fig. 2a). The displacement was recorded as the crosshead movement by the bending module. From 20 samples tested in total, 7 valid experiments were obtained and used for further analysis. Invalid experiments include cohesive failure, asymmetric crack growth, or simultaneous delamination of multiple interfaces and were not used in the

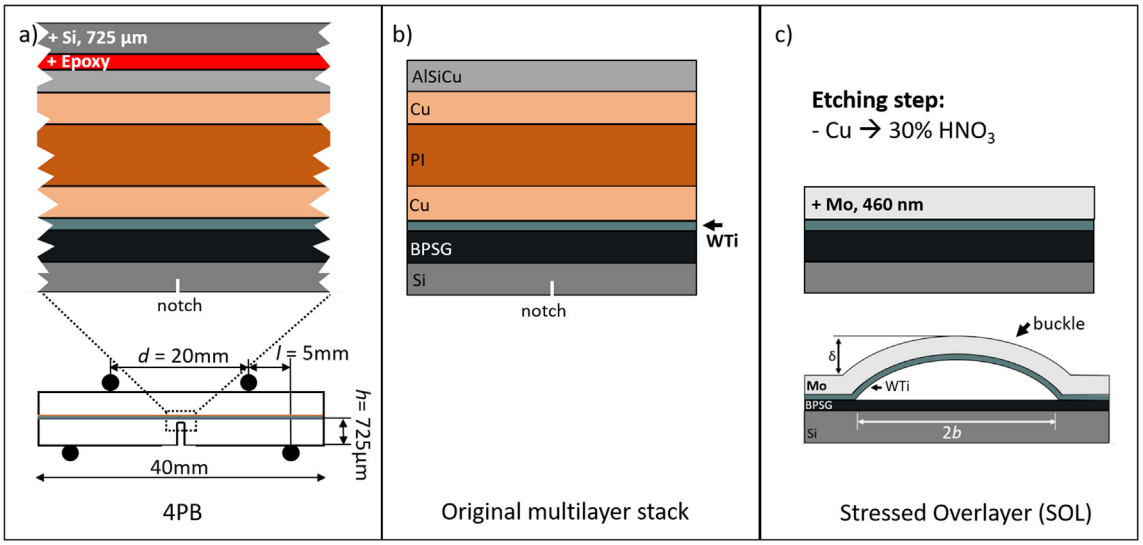

Fig. 1. Designed multimaterial stacks including schematics of the adhesion measurement techniques: a) Four point bending (4PB), b) original material stack and c) stressed overlayer method (SOL). The investigated interface is WTi-BPSG.

adhesion measurement. Schematics of failed experiments and fracture surfaces are shown in the supplementary material (Fig. S1 and S2).

2.3. Stressed overlayer method (SOL)

To cause spontaneous delamination at the WTi-BPSG interface the deposition of a stressed overlayer was necessary. Therefore, the multilayer stack was soaked in 30% HNO_3 to dissolve the Cu layers, which allowed direct access to the WTi layer without inducing mechanical damage. The sample preparation steps are schematically shown in Fig. 1c. After etching, highly stressed Mo layers with a total thickness of 460 nm (as confirmed by confocal laser scanning microscopy, not shown here) were sputter deposited onto the WTi layer in a lab-scale unbalanced dc magnetron sputtering chamber with a base

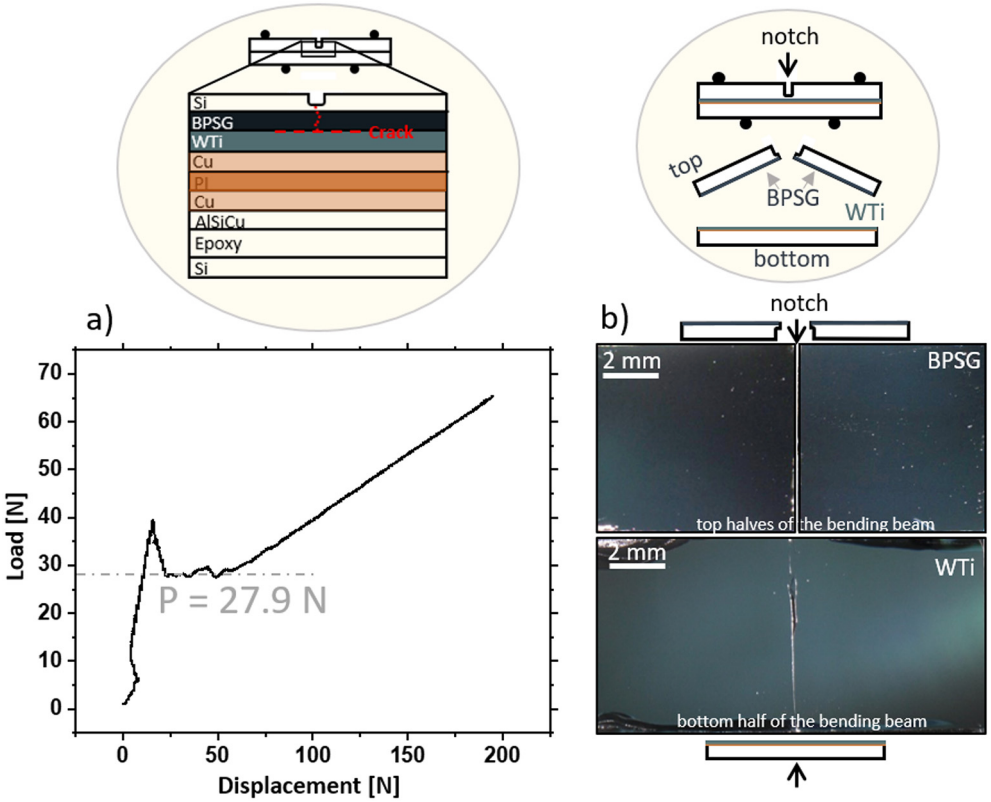

Fig. 2. Adhesion measurement of the WTi-BPSG interface with 4PB. a) Representative load-displacement curve during 4PB and schematic of the 4PB setup showing the crack propagation path. The load plateau (27.9 N) corresponding to stable, symmetric crack propagation along the WTi-BPSG interface is indicated with a dotted line. b) Failure surfaces of the sample after 4PB revealing BPSG and WTi at the top and the bottom half, respectively. The position of the notch is indicated.

pressure $< 10^{-4}$ Pa. The deposition was performed with one 2″ diameter circular target (Mo 99.97% purity) in a confocal arrangement and samples mounted on a rotatable sample holder with a target-to-substrate distance of 40 mm. Substrates were cleaned in an ultrasonic bath of isopropanol for 5 min. Prior to deposition, the target was sputter cleaned (0.1 A current) in pure Ar for 60 s, with closed target shutters to protect the substrates. Simultaneously, an asymmetrically pulsed dc bias (350 V, 50 kHz, 500 ns) was applied to the substrate to improve adhesion through plasma etching without damaging or removing the WTi layer. Mo overlayers were deposited in Ar atmosphere with a working pressure of 0.36 Pa and no intentional substrate heating. A current of 0.35 A was applied to the Mo target and a bias of 100 V was applied to the substrates during deposition, yielding a deposition rate of 0.55 nm/s.

Once the samples were covered with the Mo SOL, spontaneous local delamination at the WTi-BPSG interface was achieved in the shape of telephone cord buckles. These buckles were imaged with a confocal laser scanning microscope (CLSM, Olympus LEXT 4100 OLS). The mixed mode interfacial fracture energy $\Gamma(\Psi)$ was calculated from the Hutchinson and Suo model [32]. From the CLSM images the critical buckle parameters (half width b, height δ) were measured using Gwyddion [33]. The delaminating interface was confirmed by means of cross-sectional focused ion beam (FIB) cuts using a Zeiss LEO 1540 X dual beam workstation. Cross-sectioning was performed using two coarse cuts with 1 nA and 500 pA, followed by a final polishing step with 100 pA.

2.4. Film stress measurements

X-ray diffraction (XRD) analysis was used to investigate the residual lattice strains in the WTi layer and the Mo overlayers as a function of layer setup (4PB vs. SOL). At the KMC-2 beamline [34] (synchrotron radiation, Helmholtz-Zentrum Berlin, BESSY II) a Bruker VÅNTEC 2000 area detector was employed to record the 110 Bragg peaks of WTi and Mo in reflection geometry with a beam size of 300 μm^2, exposure times of 11 s and a wavelength of 0.154 nm. Residual lattice strains were measured with the $\sin^2\psi$ method [35] using 11 different ψ angles between 0 and 45 degrees. A Pearson fit was applied to determine peak positions and peak widths. Film stresses were calculated using X-ray elastic constants (XECs) (1/2 S2) [36] for untextured 110 WTi and 110 Mo reflections. XECs for WTi were taken from Kleinbichler et al. [37], who experimentally determined 1/2 S2 of WTi barrier layers following the procedures described in [38]. For Mo, XECs were calculated from single-crystal elastic constants assuming the Hill model with the software ElastiX [39].

3. Results

3.1. Four-point bending (4PB)

The 4PB method allows for the testing of the complete multilayer structure and identification of the weakest interface, including determination of the interface adhesion energy. Within the investigated multilayer stack, WTi-BPSG was the interface which delaminated during the 4PB test. The interface energy release rate G_i of WTi-BPSG, equivalent to adhesion energy, was calculated from the load-displacement curves obtained during 4PB. A representative load-displacement curve is shown in Fig. 2a. The peak load around 40 N corresponds to breaking of the pre-existing notch in the Si substrate. Subsequently, the crack kinks into the WTi-BPSG interface and travels symmetrically along the interface at a constant load (plateau). The crack propagation path during bending is indicated in the schematic cross-section of the multilayer stack above. The potential influence of the layer arrangement on the observed crack propagation path will be discussed in detail in Section 4. Fig. 2b shows optical microscopy images of representative fracture surfaces after testing. To facilitate interpretation, a schematic of the 4PB test and the different parts of the bending beam obtained after testing is shown above. At the top (notched wafer) and bottom halves of the tested 4PB beam BPSG and WTi are visible, respectively. Visual inspection of the fracture surfaces shows that the crack propagates homogenously along the WTi-PBSG interface, except for small areas along the edge of the sample, where delamination occurs simultaneously at multiple interfaces. The area of this disturbed edge zone is very small compared to homogeneous WTi-BPSG delamination in the center of the beam, with no significant contribution to the measured load plateau. For comparison, fracture surfaces of an invalid 4PB test, where the crack propagated simultaneously along multiple interfaces, are shown in the supplementary material (Fig. S2). With 7 out of 20 samples fulfilling the requirement of symmetric crack growth and a load plateau, the success rate of the 4PB tests is satisfactory compared to literature [30].

Using the plateau load (calculated average: $P = (27.5 \pm 0.9)$ N), the interface energy release rate G_i was calculated as (9.4 ± 0.6) J/m^2 with the following Eq. (1) [28]:

$$G_i = \frac{21(1-\nu^2)P^2l^2}{16Eh^3b^2} \quad (1)$$

where b equals the sample width (7 mm), h the half sample height, l the distance between inner and outer pins (5 mm), $\nu = 0.28$ the Poisson's ratio for Si (100) [40] and $E = 130$ GPa the Young's modulus of Si (100) [40]. For thin film multilayers constrained between two thick Si substrates, the elastic properties of Si are dominant and the elastic properties of the thin films can be disregarded [28,30]. Similarly, h was approximated as the thickness of the Si substrate (725 μm). The mean value and standard deviation for P and G_i were calculated from the 7 valid experiments. Identification of the failing interfaces was carried out via visual inspection of the fracture surfaces after testing (Fig. 2b) based on the distinctly different color and appearance of the adjacent layers (WTi, BPSG, Cu, PI, etc.).

3.2. Stressed overlayers (SOL)

To investigate the influence of adjacent layer interaction on the adhesion energy of WTi to BPSG the top layers were removed by dissolving the Cu layer in 30% HNO_3 (Fig. 1c), leading to a contact free separation of the multilayer stack into two pieces: part 1 consists of the multilayer stack Si, BPSG and WTi and the detached part 2, consisting only of PI since HNO_3 attacked the Cu and AlSiCu layers. Si, BPSG and WTi are inert against HNO_3: Consequently, this approach allows accessing of the WTi layer without mechanically or thermally changing the interface and excludes possible pre-damaging of the investigated layer. Subsequently, spontaneous delamination of the WTi layer from the BPSG substrate was triggered by means of a highly compressively stressed Mo overlayer (SOL) deposited on top of the WTi. Without the Mo SOL, no spontaneous delamination of WTi was observed. Likewise, nanoindentation or scratch testing on WTi did not trigger any delamination (not shown here). The determination of adhesion by means of stressed overlayer was first proposed by Bagchi and Evans [41]. The quantitative assessment of adhesion by means of this method was then further developed by Kriese et al. [11] based on the models by Hutchinson and Suo for spontaneous buckles [32] and the extension for spontaneously delaminating bilayers. In order to obtain sufficiently high compressive residual stresses in the sputtered Mo films leading to a delamination of the WTi-BPSG interface, a parameter study was performed on Si substrates including variation of the current applied to the target and Ar pressure during deposition. The final parameters reported in this study resulted in compressive stresses in the Mo film of approximately −3 GPa when deposited on the Si substrate, measured with XRD. The same deposition parameters were then used for the Mo stressed overlayers on top of the WTi films.

Delamination at the WTi-BPSG interface occurred in the shape of the telephone cord buckle morphology [42]. A CLSM height image of a representative buckle is shown in Fig. 3a. When the characteristic buckle dimensions (width $2b$, height δ) of the telephone cord buckles are measured at the point of inflection as shown in Fig. 3b, the buckles can be treated like straight buckles [42]. FIB cross-sections through a buckle, as shown in Fig. 3c, enable to identify the delaminating interface as WTi-BPSG. It is important to note here, that for some buckles cracking along the side of the telephone cord was observed. For adhesion analysis only buckles without cracks were considered.

When spontaneous delamination occurs with a stressed overlayer, the model of Hutchinson and Suo needs to be extended to a bilayer model considering the different stiffnesses of the involved film materials. Therefore, the critical buckling stress, σ_B, can only be determined by computing the moment of inertia, I_T, of this bilayer system, according to [11]:

$$I_T = \sum_{i=1}^{2} \frac{1}{12} n_i k h_i^3 + n_i k h_i (\overline{Y} - y_i)^2, \tag{3}$$

where $\overline{Y}$ is the composite centroid, considering the different moduli E_i of the films, y_i is the centroid and h_i is the film thickness of each individual layer, respectively. In Eq. (3), n is necessary to account for the disparate Young's moduli of the delaminated films (i.e. E_{Mo} and E_{WTi}). The variable k will cancel out once the critical buckling stress, σ_B, is computed using Eq. (4). For a deeper understanding, the reader is referred to reference [11]. The critical buckling stress, σ_B, can be obtained by

$$\sigma_B = \frac{\pi^2}{khb^2} \left[\frac{E_1}{1-\upsilon_1^2} \right] \cdot I_T, \tag{4}$$

where E_1 is the Young's modulus and ν_1 is the Poisson's ratio of the Mo film. The driving stress, σ_D, is then analogous to the Hutchinson and Suo model [32].

$$\sigma_D = \sigma_B \cdot \left[\frac{3}{4} \cdot \left(\frac{\delta}{h} \right)^2 + 1 \right], \tag{5}$$

where δ is the buckle height and h is the total film thickness of the involved layers. Finally, the mixed mode adhesion energy $\Gamma(\Psi)$ for straight sided buckles can be computed according to the well-known Hutchinson and Suo model [32] for straight sided buckles:

$$\Gamma(\Psi) = \left[\frac{(1-\nu^2)h}{2E} \right] (\sigma_d - \sigma_b)(\sigma_d + 3\sigma_b), \tag{6}$$

where h is the total film thickness, E is the thickness weighted modulus and ν is the thickness weighted Poisson's ratio of the bilayer. The phase angle of loading, Ψ, corresponds to the ratio of Mode I and Mode II loading modes during buckling and can be estimated using

$$\Psi = \tan^{-1} \left[\frac{4\cos\omega + \sqrt{3}\xi \sin\omega}{-\sin\omega + \sqrt{3}\xi \cos\omega} \right], \tag{7}$$

where ω is typically 52.1° and $\xi = \delta/h$.

Buckles without cracks were measured using CLSM height images at the point of inflection, as indicated by the orange line in Fig. 3a. Following the mechanics presented in Eq. (3)–(7) a mixed mode adhesion energy $\Gamma(\Psi) = (10.1 \pm 1.0)$ J/m^2 was computed. The results for the buckling WTi Mo SOL bilayer system are listed in Table 1. The obtained adhesion value is in good agreement with the result obtained from 4PB (9.4 ± 0.6) J/m^2 in section 3.1. Using Eq. (7) a Ψ angle of loading of 80° could be estimated for the WTi Mo SOL buckles, leading to a mode II/mode I ratio of almost 6 at the point of inflection of the telephone cord buckles. It can be concluded that a predominant shear loading mode is present for the delaminating films via Mo SOL, at the point of inflection, where adhesion was measured. This result (predominant shear loading during buckling driven delamination) is in agreement with finite element simulations of the Ψ angle of loading along the telephone cord buckle front by Faou et al. in [43]. As stated by Brinckmann et al. [44] a successful 4PB test (where the crack propagates horizontally, symmetrically along the interface of interest) implies a dominant mode II loading of the crack tip during delamination. FEM simulations by Lederer et al. confirmed that 4 PB with dominant shear loading (mode II) implies a crack bifurcation at 90° from the original notch, which again confirms that delamination by 4PB has to occur by dominant shear loading [45]. In contrast, mode I would result in cohesive cracks through the layers, which would fail to quantify interface adhesion.

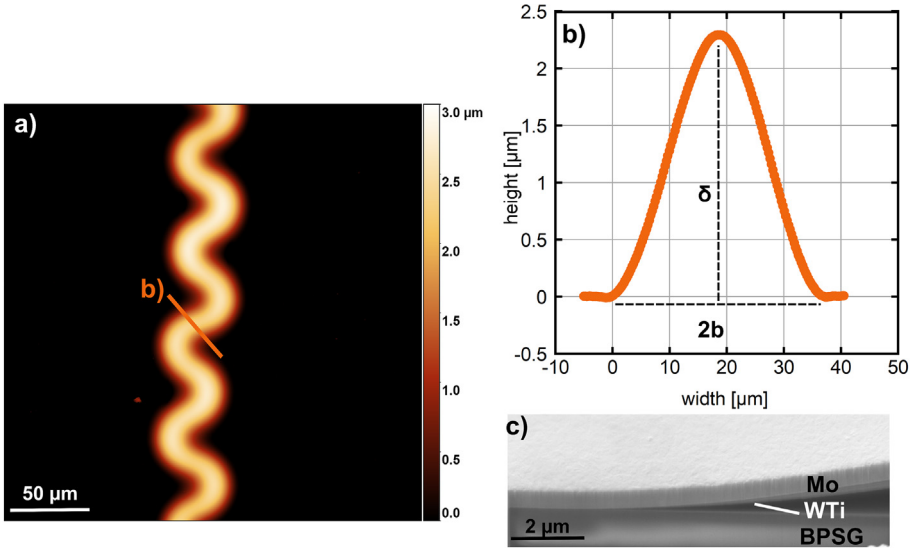

Fig. 3. Delamination of WTi-BPSG due to Mo SOL a) CLSM height image of spontaneously formed telephone cord buckle (top view). The orange line shows how the buckle dimensions were measured and b) shows the corresponding extracted buckle profile revealing buckle height, δ, and buckle width, $2b$. The position of the profile is indicated in (a) with an orange line. c) FIB cross-section of onset of telephone cord buckle highlighting delamination of WTi and Mo SOL from the BSPG layer.

Table 1
Overview of average buckle dimensions (half buckle width b, height δ), mechanical properties of WTi (subscript 1) and Mo overlayer (subscript 2).

b (μm)	δ (μm)	h_1 (nm) WTi	E_1 (GPa) WTi	ν_1 WTi	h_2 (nm) Mo	E_2 (GPa) Mo	ν_2 Mo	σ_B (GPa)	Ψ (°)
18.13 ± 0.73	2.23 ± 0.06	50	322	0.288	460	329	0.33	230 ± 12	79.95

It can therefore be concluded, that due to the similar loading modes (marked shear loading) during delamination achieved by 4PB and SOL, the obtained adhesion values can be compared.

3.3. Stress evolution within WTi as a function of neighboring layers

When comparing the WTi-BPSG adhesion results from both presented measurement techniques, it is necessary to point out that different layer architectures were present for the WTi layer. During 4PB the entire multilayer stack was tested integrally, while for the SOL technique the multilayer stack needed to be separated by etching to directly access the WTi layer before coating with Mo. Therefore, the stress state of the WTi layer was measured as a function of layer setup with XRD and the $\sin^2\Psi$ method.

In the original multilayer stack (Fig. 1b), the WTi layer had highly compressive stresses of (−1337 ± 24) MPa. After etching, when only WTi is present on the BPSG substrate (Fig. 1c before Mo deposition), the stresses in the WTi layer were measured as (−1470 ± 30) MPa. It can be concluded that removal of the top layers did not significantly alter the WTi stress state. Stress measurements of sputter deposited 300 nm WTi films in the as-deposited state with 20 at.% Ti also found highly compressive stresses of −1600 MPa [37], similar to the 50 nm WTi films of this study. In the SOL geometry (Fig. 1c) the Bragg peaks of Mo ($2\theta = 40.15°$) and WTi ($2\theta = 39.90°$) overlap. Due to this overlap of the Mo and the WTi signal, it was not possible to unambiguously measure WTi stresses in the SOL geometry. A peak deconvolution approach based on Rietveld refinement indicates that the WTi stresses in the SOL geometry are compressive, even though no precise stress value can be stated with reasonable certainty. It can be assumed that the stress state of WTi is of similar nature (approximately −1300 to −1400 MPa) in both testing geometries (4 PB and SOL), allowing direct comparison of the obtained adhesion results.

Despite the overlapping XRD signal, the difference in the peak intensity between Mo (2.5 a.u.) and WTi (0.25 a.u.) as a results of the different film thicknesses (460 nm Mo, 50 nm WTi) allowed for the investigation of the stress state of the Mo overlayer. Due to a slight texture of the Mo SOL, only a reduced number of Ψ angles for which the 2θ position of the Mo Bragg peak can be approximated by the position of the sum peak of Mo and WTi (peak intensity ratio Mo:TiW > 5:1), were considered for $\sin^2\Psi$ analysis. Measurements of the Mo stresses were performed in a flat region without buckles and in a region where buckle formation was observed. In the flat region, the Mo stresses were measured as (−1859 ± 101) MPa. In the buckled region, the Mo stresses were measured as (65 ± 183) MPa. As the size of the X-ray beam (300 μm^2) is larger than the width of a buckle (~ 40 μm, Fig. 3b) the measurements provide an average stress value over multiple buckles. Thus, buckling caused a significant relaxation of stresses in the Mo overlayer, as expected. It can also be observed that deposition onto the WTi-BPSG stack reduced the initial stress in the Mo layer (−1859 MPa) compared to the same film deposited onto Si (−3000 MPa). This effect is due to the difference in thermal expansion coefficients for Si ($\alpha_{si} = 2.5 \times 10^{-6}\,°C^{-1}$) and WTi (for comparison purposes estimated as W, $\alpha_W = 4.5 \times 10^{-6}\,°C^{-1}$) [46], which will result in different thermal stresses even with the same deposition conditions [47]. The Mo film growth is expected to be different on the electrically well conducting WTi and the semi-conducting Si (with probably SiO_2) and thus it may be manifested as a change in the stress state.

4. Discussion

In this study two techniques to determine the adhesion energy of the same WTi-BPSG interface are presented and discussed. Advantages of the 4PB technique include that the entire multilayer stack can be used and only little modification of the sample (gluing of a Si counterpart on top) is required. However, sample preparation is time-consuming, the yield of valid experiments can be very low (here, 7 out of 20) and annealing during the preparation of the 4PB beams needs to be taken into account for materials sensitive to thermal treatments, such as unannealed BPSG [23].

In principle, the method integrally allows to determine the weakest interface of a specific multilayer stack or device. However, especially in the system presented here, it can be difficult to interpret the results if several interfaces delaminate simultaneously or if there is a deviation of the exemplary crack path. Regarding the crack propagation path for 4PB adhesion measurements, our results highlight the importance of the layer order and arrangement within the multilayer stack. While 4PB was able to accurately determine the adhesion energy of the WTi-BPSG interface (9.4 ± 0.6)J/m^2, there is evidence that the method failed to identify and yield delamination of the weakest interface within the entire stack (Fig. 1b). For instance, the adhesion energy of Cu-Polyimide was determined as (6.5 ± 1.0) J/m^2 during subsequent 4PB of multilayer stacks with a slightly modified layer arrangement as compared to Fig. 1b. Even though the identical Cu-PI interface is present in the investigated stack (sputter deposited Cu on Polyimide, Fig. 1b) and the adhesion energy is expected to be significantly lower compared to WTi-BPSG, delamination during successful 4PB tests was observed predominantly along the WTi-BPSG interface as a result of the layer arrangement. While Cu-PI might therefore be a weaker interface and the weakest interface technically still remains unknown, comparison to SOL results (10.1 ± 1.0) J/m^2 ensures that the obtained 4PB adhesion energy of WTi-BPSG is accurate and valid, as further detailed in the following paragraphs. While 4PB remains a valuable technique to integrally test adhesion in multilayer stacks, the influence of layer arrangement on crack propagation through individual layers and along different interfaces needs to be critically assessed in order to correctly identify the weakest interface within the full stack, for mechanical loading conditions dissimilar to the applied 4PB or device reliability more generally. Thereby, finite element simulations [18] can be a useful tool yet requiring accurate knowledge of elastic constants of all individual layers. The presented SOL technique offers a powerful alternative to cross-check and determine adhesion energies of specific interfaces of interest.

The obtained energy release rate of 9.4 J/m^2 with 4PB is higher than values reported elsewhere. Völker et al. [30] determined energy release rates of around 6 J/m^2 for 300 nm WTi layers (Ti content 15-20 at.%) on annealed BPSG (900 °C) with a similar 4PB approach. In another 4PB study the interfacial energy release rate of 200 nm WTi on BPSG is reported as 4.9 J/m^2 [23]. In both cases, the main differences compared to this study are the WTi layer thickness and amount of Ti, if the BPSG was annealed or not, and having only one additional 500 nm AlSiCu layer. The increased adhesion energy obtained with the results presented here could be due to the thinner WTi layer (50 nm) or differences in the multilayer stack. The 4PB interface strength also includes plastic deformation in the adjacent layers, such as polyimide, Cu, AlSiCu and the epoxy layer, hence, possibly overestimating the energy needed to fracture the WTi-BPSG interface and giving an upper bond of the actual interface bond strength. Energy dissipation via plastic deformation

in the Cu and PI layers can explain the increased values obtained in this study. However, because of the good agreement between the 4PB and the SOL results, the influence of plasticity in the additional layers is considered to be marginal and the WTi film thickness may be the important factor.

When the adhesion of one specific interface is required, the SOL technique is a very precise and local method. The challenge of this technique is to directly access the interface of interest when implemented in a multi-material stack. In the material system investigated here this could be solved successfully by etching away the Cu layers, separating the multi-stack into two parts without any mechanical impact on the layers to be tested. An additional challenge for this investigation is the deposition of a highly stressed and stiff overlayer on top of the WTi, necessary to cause the desired spontaneous delamination. The fact that without a SOL no spontaneous or induced delamination (nanoindentation, scratch testing) was observed indicates good adhesion of the WTi-BPSG interface.

Compared to literature, the values measured with the SOL method are also higher than what has been previously reported for the WTi-BPSG system using similar techniques. Kleinbichler et al. [22] studied the adhesion of 300 nm sputtered WTi layer with 20 at.% Ti on BPSG. It was reported that the WTi layers delaminated from the BPSG spontaneously, but this could also be triggered by means of scratches and indents leading to mixed mode adhesion energy of 2.5 J/m^2 (for unannealed BPSG). However, after annealing the 300 nm WTi film and inducing scratch buckles, the adhesion energy was found to increase to 4.7 J/m^2 [37]. Again, the only factor that is significantly different is the thickness of the WTi layer, further illustrating that film thickness could, in fact alter the interface adhesion energies for the same interface. The fact that the WTi films did not delaminate spontaneously in the multilayer stacks studied here qualitatively indicates improved adhesion.

There is a good agreement between the WTi-BPSG adhesion energy values obtained from the different measurement techniques: (9.4 ± 0.6) J/m^2 (4PB) and (10.1 ± 1.0) J/m^2 (SOL). A dominant shear loading mode during delamination could be confirmed by both methods, (computation of Ψ angle of loading of 80° for the telephone cord buckle and a dominant shear loading mode is the condition for a successful delamination via 4PB) hence, a direct comparison of the adhesion data for the same interface is valid. Both adhesion energies are higher than values reported in literature for similar interfaces. For 4PB, the measured WTi-BPSG interface strength also includes the plastic deformation in the adjacent layers, such as Cu, PI, AlSiCu and the epoxy layer, which could explain the increased adhesion energy. However, a similarly high energy is obtained with SOL, where all of the above-mentioned layers were etched away prior to testing and the film thickness could be more important than initially believed for adhesion measurements. Therefore, the effect of adjacent layer plasticity during 4PB is considered to be small. In a previous study, Lee et al. [48] compared telephone cord buckling with 4PB for Pt films on oxidized Si substrates, which also confirms the reproducibility of both test techniques on a distinct materials system.

4PB and SOL probe interfacial adhesion at quite different spatial areas. For 4PB the delaminating area is in the order mm^2, while the area of spontaneous delaminations with SOL is in the range of a few hundred μm^2. Comparability of 4PB and SOL adhesion values can be interpreted as good lateral homogeneity of the interface. Another parameter which may be influenced by the multilayer stack geometry are the residual stresses. XRD stress measurements of the WTi layer affirm the presence of highly compressive residual stresses in the original multilayer stack and after etching away the overlying Cu film. The addition of the Mo SOL would not alter the residual stress of the WTi layer significantly. In areas, where the bilayer did not delaminate the stresses in the Mo SOL remained high (ca −1.9 GPa) and in delaminated areas the residual stress was relaxed (about 65 MPa tensile stress).

5. Conclusions

The adhesion energy of the interface between WTi and BPSG was determined with two different, quantitative measurement techniques, namely 4PB and SOL. A discussion of both test techniques allowed to justify their comparability and applicability to ultrathin metal films when implemented in a multimaterial system mimicking complex architectures in microelectronics devices. Furthermore, the comparison also highlights the importance of layer order and arrangement within the multilayer stack of interest for 4PB adhesion experiments, determining the crack propagation path and hence the apparently weakest interface. The adhesion energy obtained with 4PB tests (9.4 ± 0.6) J/m^2 is in good agreement with the results of the SOL technique (10.1 ± 1.0) J/m^2, probing a significantly smaller interface area. In both test geometries, the WTi layer has highly compressive residual stresses in the same order of magnitude and in both setups delamination occurred under predominant mode II loading, thus allowing for comparisons to be made between the two methods. The adhesion energies measured were higher than previously reported, most likely due to the 50 nm WTi thickness compared to the 200–300 nm WTi thickness in other studies. Furthermore, there is a difference as to when the BPSG layer was annealed before or after deposition of the WTi. BPSG is highly reactive in its as-deposited state which would be another influencing factor on the adhesion strength. For the case presented here, BPSG annealing was performed before the WTi layer was deposited. A final result is the direct measurement of the stress relaxation of the Mo SOL after delamination compared to an undelaminated region, yielding an on average stress-free Mo film in the buckled region. It can be concluded that in the current case, both test methods delivered reliable and meaningful values for interfacial adhesion, which is beneficial for a rapid assessment of interface stability from a design and manufacturer's perspective.

Data availability

The raw data required to reproduce the findings of this work cannot be shared at this time as the data also forms part of an ongoing study.

Declaration of Competing Interest

The authors declare that they have no known competing financial interests or personal relationships that could have appeared to influence the work reported in this paper.

Acknowledgements

This work was funded by the Austrian Science Fund (FWF) in the frame of the Hertha Firnberg program T891-N36. We thank HZB for the allocation of synchrotron radiation beam time and thankfully acknowledge the financial support by HZB (proposal 17205962-ST-1.1-P). Further funding was obtained from the EMPAPOSTDOCS-II program, which received funding from the European Union's Horizon 2020 research and innovation program under the Marie Skłodowska-Curie grant agreement number 754364.

R. Roth and P. Ganitzer from Infineon Technologies AG are gratefully acknowledged for providing the samples in this study.

Appendix A. Supplementary data

Supplementary data to this article can be found online at https://doi.org/10.1016/j.matdes.2021.109451.

References

[1] K.L. Mittal, Adhesion measurement of thin films, Electrocompon. Sci. Technol. 3 (1976) 21–42, https://doi.org/10.1155/APEC.3.21.
[2] K.L. Mittal, Adhesion Measurements of Films and Coatings, 1995.

[3] I.S. Park, J. Yu, An X-ray study on the mechanical effects of the peel test in a cu/Cr/polyimide system, Acta Mater. 46 (1998) 2947–2953, https://doi.org/10.1016/S1359-6454(97)00208-5.
[4] P.G. Charalambides, J. Lund, A.G. Evans, R.M. McMeeking, A test specimen for determining the fracture resistance of bimaterial interfaces, J. Appl. Mech. Trans. ASME. 56 (1989) 77–82, https://doi.org/10.1115/1.3176069.
[5] Q. Ma, H. Fujimoto, P. Flinn, V. Jain, F. Adibi-Rizi, F. Moghadam, R.H. Dauskardt, Quantitative measurement of interface fracture energy in multi-layer thin film structures, Mater. Res. Soc. Symp. Proc. 391 (1995) 91–96, https://doi.org/10.1557/proc-391-91.
[6] R.H. Dauskardt, M. Lane, Q. Ma, N. Krishna, Adhesion and debonding of multi-layer thin film structures, Eng. Fract. Mech. 61 (1998) 141–162, https://doi.org/10.1016/S0013-7944(98)00052-6.
[7] Z. Gan, S.G. Mhaisalkar, Z. Chen, S. Zhang, Z. Chen, K. Prasad, Study of interfacial adhesion energy of multilayered ULSI thin film structures using four-point bending test, Surf. Coat. Technol. 198 (2005) 85–89, https://doi.org/10.1016/j.surfcoat.2004.10.036.
[8] J.D. Yeager, D.J. Phillips, D.M. Rector, D.F. Bahr, Characterization of flexible ECoG electrode arrays for chronic recording in awake rats, J. Neurosci. Methods 173 (2008) 279–285, https://doi.org/10.1016/j.jneumeth.2008.06.024.
[9] A.A. Volinsky, N.R. Moody, W.W. Gerberich, Interfacial toughness measurements for thin films on substrates, Acta Mater. 50 (2002) 441–466, https://doi.org/10.1016/S1359-6454(01)00354-8.
[10] D.B. Marshall, A.G. Evans, Measurement of adherence of residually stressed thin films by indentation. I. Mechanics of interface delamination, J. Appl. Phys. 56 (1984) 2632–2638, https://doi.org/10.1017/CBO9781107415324.004.
[11] M.D. Kriese, W.W. Gerberich, N.R. Moody, Quantitative adhesion measures of multilayer films: Part I. Indentation mechanics, J. Mater. Res. 14 (1999) 3007–3018, https://doi.org/10.1557/JMR.1999.0404.
[12] S.Y. Grachev, A. Mehlich, J.-D. Kamminga, E. Barthel, E. Søndergård, High-throughput optimization of adhesion in multilayers by superlayer gradients, Thin Solid Films 518 (2010) 6052–6054, https://doi.org/10.1016/j.tsf.2010.06.049.
[13] H. Hirakata, Y. Takahashi, D. Truong, T. Kitamura, Role of plasticity on interface crack initiation from a free edge and propagation in a nano-component, Int. J. Fract. 145 (2007) 261–271, https://doi.org/10.1007/s10704-007-9079-0.
[14] K. Matoy, T. Detzel, M. Müller, C. Motz, G. Dehm, Interface fracture properties of thin films studied by using the micro-cantilever deflection technique, Surf. Coat. Technol. 204 (2009) 878–881, https://doi.org/10.1016/j.surfcoat.2009.09.013.
[15] J. Schaufler, C. Schmid, K. Durst, M. Göken, Determination of the interfacial strength and fracture toughness of a-C:H coatings by in-situ microcantilever bending, Thin Solid Films 522 (2012) 480–484, https://doi.org/10.1016/j.tsf.2012.08.031.
[16] B. Völker, W. Heinz, R. Roth, J.M. Batke, M.J. Cordill, G. Dehm, Downscaling metal-dielectric interface fracture experiments to sub-micron dimensions: a feasibility study using TEM, Surf. Coat. Technol. 270 (2015) 1–7, https://doi.org/10.1016/j.surfcoat.2015.03.027.
[17] R. Dudek, W. Faust, A. Gollhard, B. Michel, A FE-study of solder fatigue compared to microstructural damage evaluation by in-SITU laser scanning and FIB microscopy, Therm. Thermomechanical Proc. 10th Intersoc. Conf. Phenom. Electron. Syst. 2006. ITHERM 2006 2006, pp. 1031–1037, https://doi.org/10.1109/ITHERM.2006.1645458.
[18] J.L. Mead, M. Lu, H. Huang, Microscale interfacial adhesion assessment in a multilayer by a miniaturised four-point bending test, Mech. Mater. 129 (2019) 341–351, https://doi.org/10.1016/j.mechmat.2018.12.003.
[19] R. Schoeppner, C. Ferguson, L. Pethö, C. Guerra-nuñez, A.A. Taylor, M. Polyakov, B. Putz, J. Breguet, I. Utke, J. Michler, Interfacial adhesion of alumina thin films over the full compositional range of ternary fcc alloy films : a combinatorial nanoindentation study, Mater. Des. 193 (2020) 108802, https://doi.org/10.1016/j.matdes.2020.108802.
[20] K. Matoy, H. Schönherr, T. Detzel, T. Schöberl, R. Pippan, C. Motz, G. Dehm, A comparative micro-cantilever study of the mechanical behavior of silicon based passivation films, Thin Solid Films 518 (2009) 247–256, https://doi.org/10.1016/j.tsf.2009.07.143.
[21] M.D. Kriese, N.R. Moody, W.W. Gerberich, Effects of annealing and interlayers on the adhesion energy of copper thin films to SiO2/Si substrates, Acta Mater. 46 (1998) 6623–6630, https://doi.org/10.1016/S1359-6454(98)00277-8.
[22] A. Kleinbichler, J. Zechner, M.J. Cordill, Buckle induced delamination techniques to measure the adhesion of metal dielectric interfaces, Microelectron. Eng. 167 (2017) 63–68, https://doi.org/10.1016/j.mee.2016.10.020.
[23] B. Völker, W. Heinz, K. Matoy, R. Roth, J.M. Batke, T. Schöberl, C. Scheu, G. Dehm, Interface fracture and chemistry of a tungsten-based metallization on borophosphosilicate glass, Philos. Mag. 95 (2015) 1967–1981, https://doi.org/10.1080/14786435.2014.913108.
[24] A. Kleinbichler, M.J. Pfeifenberger, J. Zechner, N.R. Moody, D.F. Bahr, M.J. Cordill, New insights into Nanoindentation-based adhesion testing, Jom. 69 (2017) 2237–2245, https://doi.org/10.1007/s11837-017-2496-2.
[25] C.S. Litteken, S. Strohband, R.H. Dauskardt, Residual stress effects on plastic deformation and interfacial fracture in thin-film structures, Acta Mater. 53 (2005) 1955–1961, https://doi.org/10.1016/j.actamat.2005.01.005.
[26] S.B. Koo, C.M. Lee, S.J. Kwon, J.M. Jeon, J. Young Hur, H.K. Lee, Study on aging effect of adhesion strength between polyimide film and copper layer, Met. Mater. Int. 25 (2019) 117–126, https://doi.org/10.1007/s12540-018-0167-7.
[27] A. Lassnig, M. Lederer, G. Khatibi, R. Pelzer, W. Robl, M. Nelhiebel, High cycle fatigue testing of thermosonic ball bonds, Microelectron. Reliab. 71 (2017) 91–98, https://doi.org/10.1016/j.microrel.2017.02.019.
[28] Q. Ma, H. Fujimoto, P. Flinn, V. Jain, F. Adibi-rizi, F. Moghadam, R.H. Dauskardt, Energy in Multi-Layer Thin Film Structures, 391, 1995 91–96.
[29] Q. Ma, J. Bumgarner, H. Fujimoto, M. Lane, R.H. Dauskardt, Adhesion measurement of interfaces in multilayer interconnect structures, Mater. Res. Soc. Symp. - Proc 1997, pp. 3–14.
[30] B. Völker, W. Heinz, K. Matoy, R. Roth, J.M. Batke, T. Schöberl, M.J. Cordill, G. Dehm, Mechanical and chemical investigation of the interface between tungsten-based metallizations and annealed borophosphosilicate glass, Thin Solid Films 583 (2015) 170–176, https://doi.org/10.1016/j.tsf.2015.03.047.
[31] P.G. Charalambides, H.C. Cao, J. Lund, A.G. Evans, Development of a test method for measuring the mixed mode fracture resistance of Bimaterial interfaces, Mech. Mater. 8 (1990) 269–283.
[32] J.W. Hutchinson, Z. Suo, Mixed mode cracking in layered materials, Adv. Appl. Mech. 29 (1991) 63–191, https://doi.org/10.1016/S0065-2156(08)70164-9.
[33] D. Nečas, P. Klapetek, Gwyddion: an open-source software for SPM data analysis, Open Phys. 10 (2012) 181–188.
[34] D. Többens, S. Zander, KMC-2: an X-ray beamline with dedicated di raction and XAS endstations at BESSY II, J. Large-Scale Res. Facil. 2 (2016) 1–6.
[35] L. Spieß, G. Teichert, R. Schwarzer, H. Behnken, C. Genzel, Moderne Röntgenbeugung, Vieweg+Teubner Verlag 2009.
[36] I.C. Noyan, J.B. Cohen, Residual Stress: Measurement by Diffraction and Interpretation, Springer-Verlag, New York, 2013.
[37] A. Kleinbichler, J. Todt, J. Zechner, S. Wöhlert, D.M. Többens, M.J. Cordill, Annealing effects on the film stress and adhesion of tungsten-titanium barrier layers, Surf. Coat. Technol. 332 (2017) 376–381, https://doi.org/10.1016/j.surfcoat.2017.07.087.
[38] E. Eiper, K.J. Martinschitz, J.M. Lackner, I. Zizak, N. Darowski, J. Keckes, X-ray elastic constants determined by the combination of sin2psi and substrate-curvature methods, Z. Met. 96 (2005) 1069–1073.
[39] H. Wern, N. Koch, T. Maas, Self-Consistent calculation of the X-ray elastic constants of polycristalline materials for arbitrary crystal symmetry, Mater. Sci. Forum 404–407 (2002) 127–132 doi:10.4028/www.scientific.net/MSF.404-407.127.
[40] J.J. Wortman, R.A. Evans, Young's Modulus, Shear Modulus, and Poisson's Ratio in Silicon and Germanium, 153, 1965https://doi.org/10.1063/1.1713863.
[41] A. Bagchi, A.G. Evans, Measurements of the debond energy for thin metallization lines on dielectrics, Thin Solid Films 286 (1996) 203–212.
[42] M.J. Cordill, D.F. Bahr, N.R. Moody, W.W. Gerberich, Adhesion measurements using telephone cord buckles, Mater. Sci. Eng. A 443 (2007) 150–155, https://doi.org/10.1016/j.msea.2006.08.027.
[43] J.Y. Faou, G. Parry, S. Grachev, E. Barthel, How does adhesion induce the formation of telephone cord buckles? Phys. Rev. Lett. 108 (2012) 1–5, https://doi.org/10.1103/PhysRevLett.108.116102.
[44] S. Brinckmann, B. Völker, G. Dehm, Crack deflection in multi-layered four-point bending samples, Int. J. Fract. 190 (2014) 167–176, https://doi.org/10.1007/s10704-014-9981-1.
[45] M. Lederer, A.B. Kotas, G. Khatibi, H. Danninger, On crack propagation in homogeneous and composite materials under mixed mode loading conditions, Procedia Struct. Integr. 23 (2019) 203–208, https://doi.org/10.1016/j.prostr.2020.01.087.
[46] W.D. Callister, Materials Science and Engineering: An Introduction, 5th ed. John Wiley & Sons, Inc, New York, 2000.
[47] M. Ohring, Mechanical properties of thin films, Mater. Sci. Thin Film, 2nd edElsevier 2002, pp. 711–781.
[48] A. Lee, C.S. Litteken, R.H. Dauskardt, W.D. Nix, Comparison of the telephone cord delamination method for measuring interfacial adhesion with the four-point bending method, Acta Mater. 53 (2005) 609–616, https://doi.org/10.1016/j.actamat.2004.10.014.